

Fluorescence spectroscopy of single-walled carbon nanotubes synthesized from alcohol

Yuhei Miyauchi, Shohei Chiashi, Yoichi Murakami, Yasunori Hayashida, Shigeo Maruyama*

*Department of Mechanical Engineering, The University of Tokyo
7-3-1 Hongo, Bunkyo-ku, Tokyo 113-8656, Japan*

Received 5 December 2003; in final form 14 January 2004

*Corresponding Author. Fax: +81-3-5800-6983.

E-mail address: maruyama@photon.t.u-tokyo.ac.jp (S. Maruyama).

Abstract

Near-infrared fluorescence measurements were performed on single-walled carbon nanotubes (SWNTs) catalytically synthesized from alcohol under various experimental conditions (alcohol catalytic CVD method, ACCVD). The chirality distribution was determined by measuring the fluorescence emitted from separated SWNTs as a function of excitation wavelength. Compared with HiPco SWNTs, chiralities of the ACCVD sample were distributed predominantly in the higher chiral angle region, close to the so-called armchair structure. This tendency toward higher chiral angles was more pronounced for smaller diameter nanotubes. The reason for the armchair-rich chirality distribution is discussed based on the initial cap structure satisfying the ‘isolated pentagon rule’.

1. Introduction

Since their discovery in 1993 [1], single-walled carbon nanotubes (SWNTs) have attracted much attention as a new material with numerous possible applications [2] due to their unique physical properties [3]. In addition to the laser-furnace [4] and arc-discharge [5] techniques, various catalytic chemical vapor deposition (CCVD) methods [6-12] including the high-pressure CO (HiPco) technique [7, 8] have been proposed for possible low-cost large scale production. At present, CCVD methods have become major approaches for mass production of SWNTs. However, CCVD synthesis of high-quality SWNTs still suffers from problems with metal particle and amorphous carbon impurities contained in the products. As a possible solution to this problem, we have proposed a catalytic CVD technique using alcohol as the carbon source [13, 14]. This

so-called alcohol catalytic CVD (ACCVD) method has been shown to produce high-quality SWNTs at temperatures as low as 550°C when combined with appropriate catalysts.

For the development of electronic and optical applications of SWNTs, structure-controlled synthesis of SWNTs is eagerly anticipated because electronic and optical properties of SWNTs depend on their chirality structure, which is designated by two integers (n , m) [3]. Due to the lack of techniques for measuring the structure distribution of bulk SWNTs, the effects of various experimental conditions on a synthesized nanotube's structure remain unresolved. However, the recent breakthrough in spectrofluorimetric measurement [15, 16] has opened the door to a quick determination of the structure distribution in a bulk SWNTs sample.

In this report, chirality distributions of SWNTs synthesized by ACCVD under various experimental conditions are compared by a spectrofluorimetric analysis [17]. SWNTs synthesized by this method are found to be rich in near-armchair type nanotubes, especially for tubes with small diameters.

2. Experimental

Zeolite-supported metal catalyst was prepared using the reported procedure [13, 14]. Iron acetate $[(\text{CH}_3\text{CO}_2)_2\text{Fe}]$ and cobalt acetate $[(\text{CH}_3\text{CO}_2)_2\text{Co}\cdot 4\text{H}_2\text{O}]$ were impregnated into USY-zeolite powder [HSZ-390HUA from Tosoh] [18, 19]. The amounts of Fe and Co were 2.5 wt % each, with respect to the zeolite powder. The catalyst was placed in a quartz boat, which was set in a quartz tube (i.d. 27 mm) inside an electric furnace [14]. During heating by the electric furnace, 300 sccm (standard cc/min) of Ar/H₂ (3 % H₂) was supplied so as to maintain the pressure inside the quartz tube at 300 ± 20 Torr. After the electric furnace reached the growth temperature, Ar/H₂ was stopped, and the quartz tube was evacuated by a rotary pump. Ethanol vapor from a reservoir was then introduced for 10 min at a constant pressure of 10 Torr. After completion of the CVD reaction, the electric furnace was turned off, and 100 sccm of Ar/H₂ was flowed through the tube while it cooled to room temperature.

In order to perform a spectrofluorimetric measurement, samples rich in individual SWNTs in surfactant suspension were prepared by a procedure similar to O'Connell et al. [15]. The 'as grown' sample was dispersed in D₂O with 1 wt % sodium dodecyl sulfate (SDS) by heavy sonication with an ultrasonic processor (Hielscher GmbH, UP-400S with S3/Micro Tip 3) for 1 h at a power flux level of 460 W/cm². This suspension was then centrifuged (SIGMA Laborzentrifugen GmbH, 2-16 with s12148 angle rotor) for 24 h at 20627 g and the supernatant, rich in isolated SWNTs, was used in the measurement.

In addition to spectrofluorimetric measurements, the synthesized SWNTs were characterized

by resonant Raman scattering and optical absorption. The Raman spectra were measured using a CHROMEX 501is spectrometer, an ANDOR Technology DV401-FI CCD system, and a SEKI TECHNOTRON Corp. STR250 optical system. The VIS-NIR absorption spectra were measured with a HITACHI U-4000. The fluorescence spectra were measured with a HORIBA SPEX Fluorolog-3-11 spectrofluorometer with a liquid-nitrogen-cooled InGaAs near IR detector.

3. Results and discussion

3.1 Effect of CVD temperature on chirality distribution

Figure 1 shows optical absorption of isolated SWNTs in an aqueous surfactant suspension and Raman radial breathing mode (RBM) signals of ‘as grown’ samples. Distinct absorption peaks corresponding to the electronic band gaps [15] were observed for the isolated nanotubes prepared by our technique. The structure around 1000-1500 nm corresponds to the E_{11} band-gap of a semiconducting nanotube [20]. Since the band gap is roughly inversely proportional to the nanotube diameter, the diameter distribution of the nanotubes can be estimated. For ACCVD samples, a decrease in the temperature was accompanied by a decrease in the diameter as well as a narrowing of the diameter distribution. The observed temperature dependence of the diameter distribution is currently interpreted as follows: Thinner nanotubes are predominant at lower temperatures because the kinetic reaction path is simpler, whereas energetically stable thicker nanotubes are dominant at higher temperatures. A wider diameter distribution for the HiPco sample is also noticed. The RBM signal also gives information about the diameter distribution. Two well-known correlations between the diameter d (nm) of SWNTs and RBM Raman shift ν (cm^{-1}) are shown on the top axis of Fig. 1. The correlation $d = 248/\nu$ was proposed based on Raman scatterings by individual nanotubes [21], and the correlation $d = 223.5/(\nu-12.5)$ was proposed based on comparison with spectrofluorimetric measurements [16]. The dependence of the diameter distribution of the ACCVD samples on the reaction temperature estimated from the RBM frequency is consistent with optical absorption. However, the wider distribution and larger diameters of the HiPco sample compared with the ACCVD sample are not clearly distinguishable by the RBM signal because of the strong resonant feature due to the van Hove singularity. Furthermore, modification of the electronic structure caused by the bundling of nanotubes may affect the resonance of the RBM mode.

Figure 2 is a contour plot comparing the fluorescence spectra of ACCVD samples grown at various CVD temperatures and the HiPco sample. Fluorescence in the 900 – 1300 nm range was recorded while the excitation wavelength was scanned from 500 to 900 nm. The measured spectral data were corrected for wavelength-dependent variations in excitation intensity and detection sensitivity. The excitation and emission spectral slit widths were both 10 nm, and scan steps were 5

nm on both axes. Each distinct peak in Fig. 2 corresponds to emission from the first band gap (E_{11}) of a semiconducting SWNT, which has first been excited to the second band gap (E_{22}). The positions of the peaks were almost identical to those in the measurements by Bachilo et al. [16], who assigned values (n, m) to each peak by comparing fluorescence spectra with Raman scattering spectra and the theoretical band gap. There is a considerable difference, however, when compared to the (n, m) assignment deduced from the Kataura plot [22], which is based on micro Raman scattering by individual nanotubes [21]. Further experimental and theoretical studies which provide a more consistent assignment are anticipated. The assignment by Bachilo et al. [16] was adopted in the present Letter to deduce the chirality distribution of our samples. Major peaks in Fig. 2 are labeled with corresponding (n, m) indices. A comparison of the spectra in Fig. 2 shows that only a few major peaks are prominent for ACCVD SWNTs [17], whereas several major peaks are present for the HiPco SWNT sample. In particular, the ACCVD sample produced at 650 °C shows only two dominant peaks corresponding to SWNTs having chiral indices (6, 5) and (7, 5).

Figure 3 shows the distributions of the diameter and the chiral angle. Since no information on the structure-dependent fluorescence quantum yield is available, the intensity of fluorescence is assumed to closely represent the abundance. An apparent difference in the chirality distribution dependent on the source of the SWNTs is observed in Fig. 3. In comparison with the HiPco sample, the ACCVD samples have smaller average diameters and narrower diameter distributions. The fluorescence spectra indicate that a decrease in the reaction temperature causes the diameter distribution of ACCVD SWNTs to shift to the thinner side, which agrees with the absorption and Raman scattering spectra shown in Fig. 1. In addition, the chiral angles of ACCVD SWNTs are predominantly distributed in the higher angle region close to the armchair type, especially in the small diameter case. HiPco SWNTs, on the other hand, show a less remarkable dependence of the distribution on the chiral angle, though a near-armchair structure distribution was initially reported for HiPco SWNTs [16]. The armchair-rich features can also be observed in the absorption spectra in Fig. 1A, where major peak features are all assigned to near-armchair nanotubes.

3.2 Effect of catalysts and alcohol source

To investigate the effects of the kinds of alcohol and the composition of the catalyst, we compared fluorescence spectra of SWNTs synthesized under different experimental conditions with a spectrum of a standard ACCVD sample, synthesized from *ethanol* at 850 °C using *Fe/Co* catalyst (2.5 wt % each). One sample was synthesized by replacing ethanol with methanol ('methanol' sample), while another sample was synthesized by replacing the bimetallic catalyst (Fe/Co 2.5 wt %) with a single-metal catalyst (Co 5 wt %) ('Co 5 wt %' sample). The CVD temperature for each sample was kept at 850 °C. Figure 4 shows the structure distributions of these two samples. In

both cases, the fluorescence peaks were found at the estimated positions corresponding to specific chiral indices (n, m), as is the case with the standard ACCVD sample (not shown). Figure 4a shows more large-diameter nanotubes were present in the methanol sample than in the ethanol sample. This shift in the diameter distribution is consistent with our previous report [13]. When methanol is used as the CVD carbon source, twice as much oxygen is involved in the reaction on the metal particle. It is suspected that the stronger oxygen effect tends to prevent the formation of less stable small-diameter nanotubes. Note that the structure distribution in the methanol sample was much less dependent on the chiral angle than the case of standard ACCVD tubes produced using ethanol, despite the use of the same catalyst. On the other hand, in the case of the 'Co 5wt %' sample shown in Fig. 4b, the structure distribution of SWNTs nearly equal to that of the standard ACCVD tubes despite the use of a different catalyst. Since the structure distribution shifts toward the armchair type only when the diameters of the SWNTs are smaller, these results suggest that the dominant factor that determines the chirality distribution of SWNTs is the diameters of the nanotubes. Furthermore, the spectrofluorimetric observations of Bachilo et al. [23] on the structure distribution of SWNTs synthesized by the Co/Mo CO-disproportional reaction CCVD method of Resasco et al., CoMo CAT [11], were remarkably similar to ours obtained from ACCVD SWNTs synthesized at 650 °C shown in Fig.2(c), with major peaks at (6, 5) and (7, 5). This similarity in the structure distributions of the ACCVD and CoMo CAT methods seems to support the idea that the near-armchair chirality distribution is primarily due to smaller diameters. The experimental conditions used by these authors, including the carbon sources and catalysts, were totally different from our ACCVD method, the only similarity being the small SWNT diameters. A careful study of the diameter distribution below 0.85 nm in Fig. 3(d) shows the abundance of near-armchair HiPco SWNTs. When macroscopic generation of SWNTs was achieved with the laser-furnace technique, the chirality distribution had been believed to be armchair-rich [4] until the direct observation of chirality of individual nanotubes was achieved by STM [24] and by micro-Raman spectroscopy [21]. The armchair-rich feature has now been confirmed for only small diameter nanotubes by more convenient spectrofluorimetric measurements.

3.3 Initial cap structure satisfying 'isolated pentagon rule'

The reason why small-diameter SWNTs tend to stabilize near-armchair structures may be interpreted by considering the stability and the number of possible cap structures corresponding to each (n, m) structure. The growth mechanism of SWNTs suggests that the initial cap structure is formed on the catalyst before subsequent growth of the tube wall [25]; hence, the chiral structure of the nanotube is determined by the initial cap structure. The number of possible cap structures for each (n, m) body has been determined by a sophisticated numerical technique [26] under the

assumption that the nanotube cap structure satisfies the isolated pentagon rule (IPR), which is the generally accepted rule for a stable fullerene structure. The number of possible cap structures for small-diameter tubes (less than 0.8 nm diameter) is very few, but increases exponentially for larger diameter tubes. For example, (6, 5) and (9, 1) nanotubes, which coincidentally have the same diameter, have a unique possible cap structure, which satisfies the IPR [26]. The (6, 5) fluorescence peak was found to be much stronger than the (9, 1) peak in all results in Fig. 3. According to our preliminary study on small diameter nanotubes, the cap structure for near-armchair nanotubes tends to be more stable than those for near-zigzag nanotubes.

Acknowledgements

The authors are grateful to Prof. R. E. Smalley (Rice University) for supplying the HiPco sample, Prof. R. B. Weisman (Rice University) for preprints, and Mr. Erik Einarsson (University of Tokyo) for discussions. Parts of this work were financially supported by KAKENHI #13555050 from JSPS and #13GS0019 from MEXT.

References

- [1] S. Iijima, T. Ichihashi, *Nature* 363 (1993) 603.
- [2] M.S. Dresselhaus, G. Dresselhaus, P. Avouris, *Carbon Nanotubes*, Springer, Berlin, 2001.
- [3] R. Saito, G. Dresselhaus, M.S. Dresselhaus, *Physical Properties of Carbon Nanotubes*, Imperial College Press, London, 1998.
- [4] A. Thess, R. Lee, P. Nikolaev, H. Dai, P. Petit, J. Robert, C. Xu, Y.H. Lee, S.G. Kim, A.G. Rinzler, D.T. Colbert, G.E. Scuseria, D. Tománek, J.E. Fischer, R.E. Smalley, *Science* 273 (1996) 483.
- [5] C. Journet, W.K. Maser, P. Bernier, A. Loiseau, M.L. de la Chapelle, S. Lefrant, P. Deniard, R. Lee, J.E. Fischer, *Nature* 388 (1997) 756.
- [6] H. Dai, A.G. Rinzler, P. Nikolaev, A. Thess, D.T. Colbert, R.E. Smalley, *Chem. Phys. Lett.* 260 (1996) 471.
- [7] P. Nikolaev, M.J. Bronikowski, R.K. Bradley, F. Rohmund, D.T. Colbert, K.A. Smith, R.E. Smalley, *Chem. Phys. Lett.* 313 (1999) 91.
- [8] M.J. Bronikowski, P.A. Willis, D.T. Colbert, K.A. Smith, R.E. Smalley, *J. Vac. Sci. Technol. A* 19 (2001) 1800.
- [9] J.-F. Colomer, J.-M. Benoit, C. Stephan, S. Lefrant, G. Van Tendeloo, J.B. Nagy, *Chem. Phys. Lett.* 345 (2001) 11.
- [10] B. Zheng, Y. Li, J. Liu, *Appl. Phys. A* 74 (2002) 345.

- [11] W.E. Alvarez, F. Pompeo, J.E. Herrera, L. Balzano, D.E. Resasco, *Chem. Mater.* 14 (2002) 1853.
- [12] A.R. Harutyunyan, B.K. Pradhan, U.J. Kim, G. Chen, P.C. Eklund, *Nano Lett.* 2 (2002) 525.
- [13] S. Maruyama, R. Kojima, Y. Miyauchi, S. Chiashi, M. Kohno, *Chem. Phys. Lett.* 360 (2002) 229.
- [14] Y. Murakami, Y. Miyauchi, S. Chiashi, S. Maruyama, *Chem. Phys. Lett.* 374 (2003) 53.
- [15] M.J. O'Connell, S.M. Bachilo, C.B. Huffman, V.C. Moore, M.S. Strano, E.H. Haroz, K.L. Rialon, P.J. Boul, W.H. Noon, C. Kittrell, J. Ma, R.H. Hauge, R.B. Weisman, R.E. Smalley, *Science* 297 (2002) 593.
- [16] S.M. Bachilo, M.S. Strano, C. Kittrell, R.H. Hauge, R.E. Smalley, R.B. Weisman, *Science* 298 (2002) 2361.
- [17] S. Maruyama, Y. Miyauchi, Y. Murakami, S. Chiashi, *New J. Phys.*, 5 (2003) 149.1.
- [18] K. Mukhopadhyay, A. Koshio, N. Tanaka, H. Shinohara, *Jpn. J. Appl. Phys.* 37 (1998) L1257.
- [19] K. Mukhopadhyay, A. Koshio, T. Sugai, N. Tanaka, H. Shinohara, Z. Konya, J.B. Nagy, *Chem. Phys. Lett.* 303 (1999) 117.
- [20] H. Kataura, Y. Kumazawa, Y. Maniwa, I. Umezumi, S. Suzuki, Y. Ohtsuka, Y. Achiba, *Synth. Met.* 103 (1999) 2555.
- [21] A. Jorio, R. Saito, J.H. Hafner, C.M. Lieber, M. Hunter, T. McClure, G. Dresselhaus, M.S. Dresselhaus, *Phys. Rev. Lett.* 86 (2001) 1118.
- [22] R.B. Weisman, S.M. Bachilo, *Nano Lett.* 3 (2003) 1235.
- [23] S.M. Bachilo, L. Balzano, J. E. Herrera, F. Pompeo, D.E. Resasco, R.B. Weisman, *J. Am. Chem. Soc.* 125 (2003) 11186.
- [24] J.W. Wildöer, L.C. Venema, A.G. Rinzler, R.E. Smalley, C. Dekker, *Science* 291 (1998) 59.
- [25] Y. Shibuta, S. Maruyama, *Chem. Phys. Lett.* 382 (2003) 381.
- [26] T. Yu. Astakhova, G.A. Vinogradov, E. Ōsawa, *Fullerene Sci. Technol.* 7 (1999) 769.

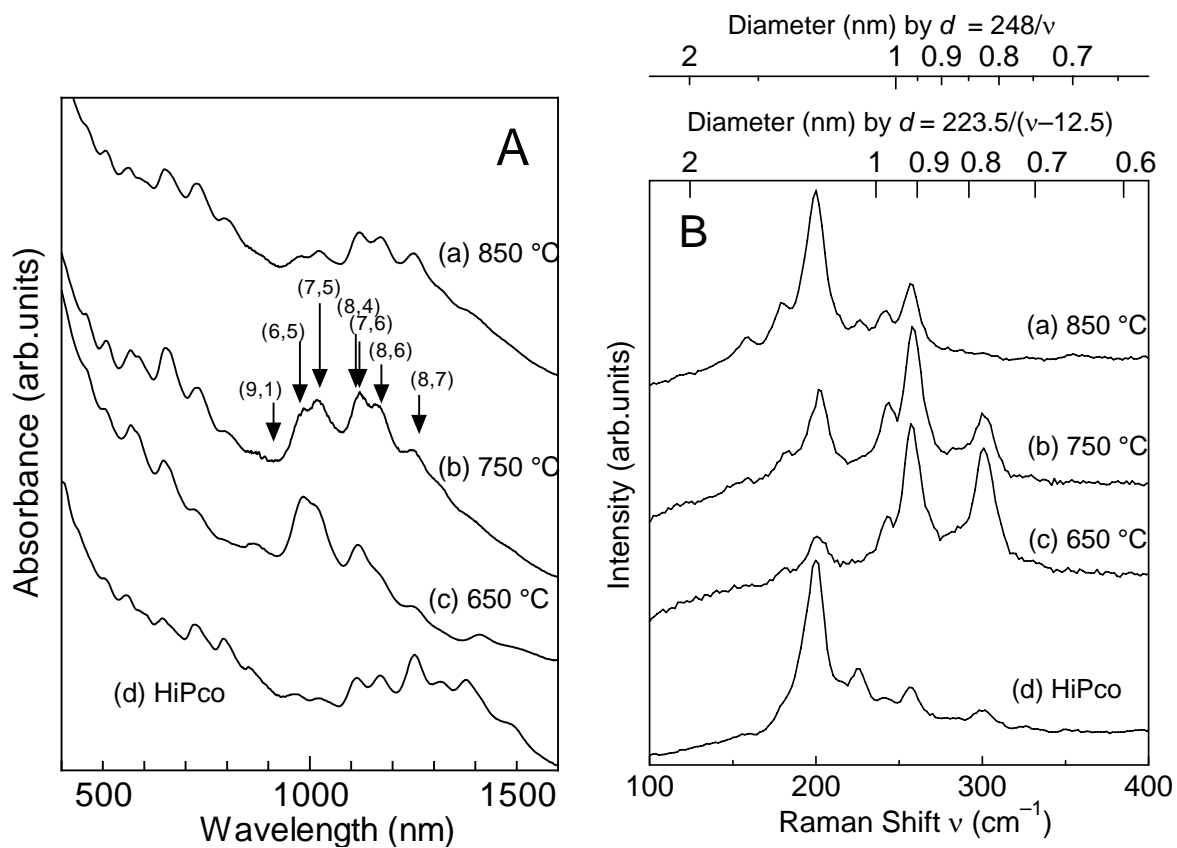


Fig. 1. (A) Optical absorption of aqueous surfactant suspension and (B) Raman RBM spectra of ‘as grown’ SWNTs measured with a 488nm excitation laser. ACCVD was performed for 10 min at the reaction temperature labeled in the figure using ethanol as the carbon source. HiPco SWNTs were supplied from Rice University (batch # HPR 113.4). Arrows and chiral indices in (A) were assigned by spectrofluorimetric measurements [16].

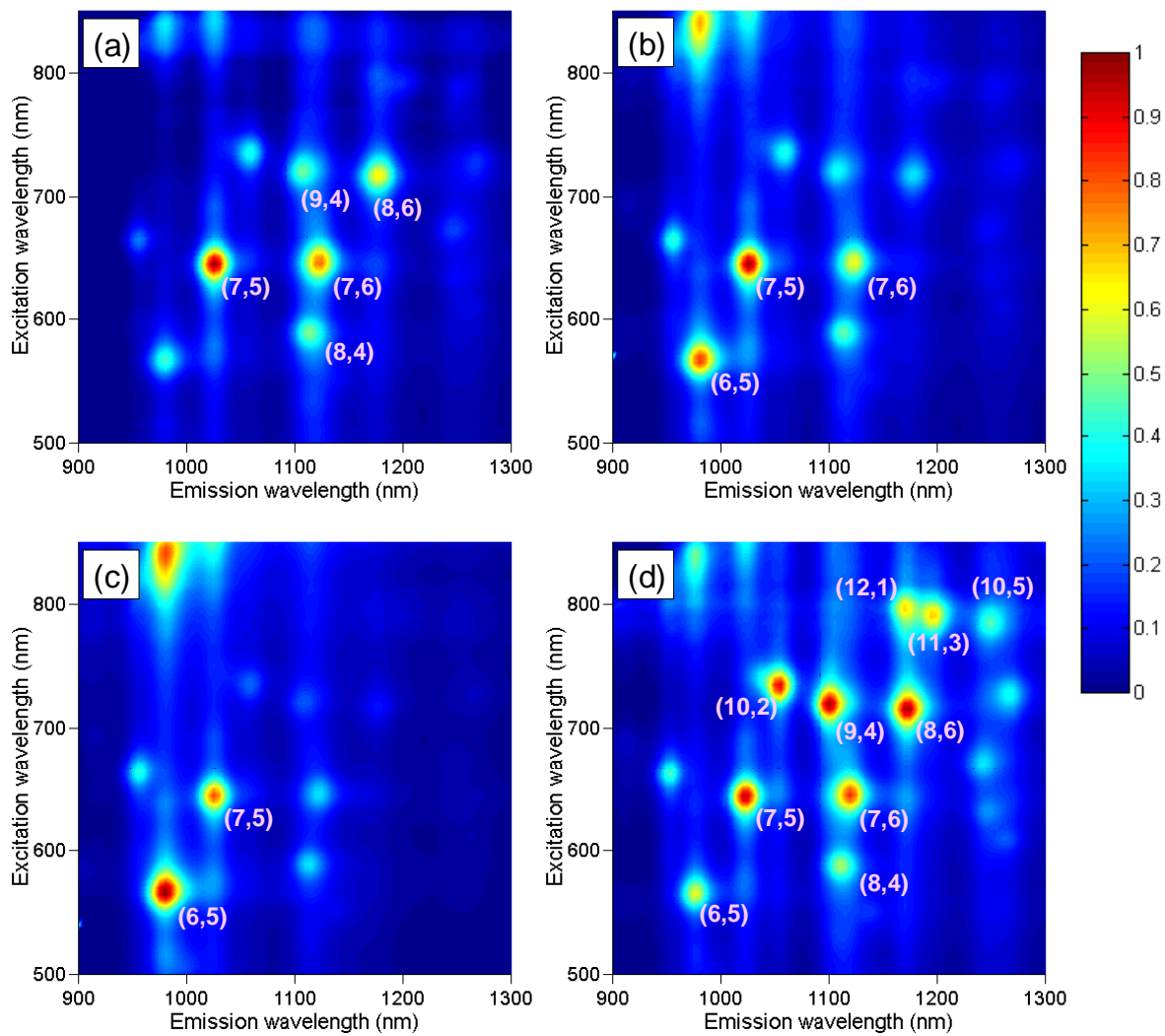


Fig. 2. Contour plots of fluorescence spectra as a function of excitation wavelength and the resultant emission. The samples used for this measurement are the same as those used for the optical absorption in Fig. 1. (a) 850 °C, (b) 750 °C, (c) 650 °C, (d) HiPco.

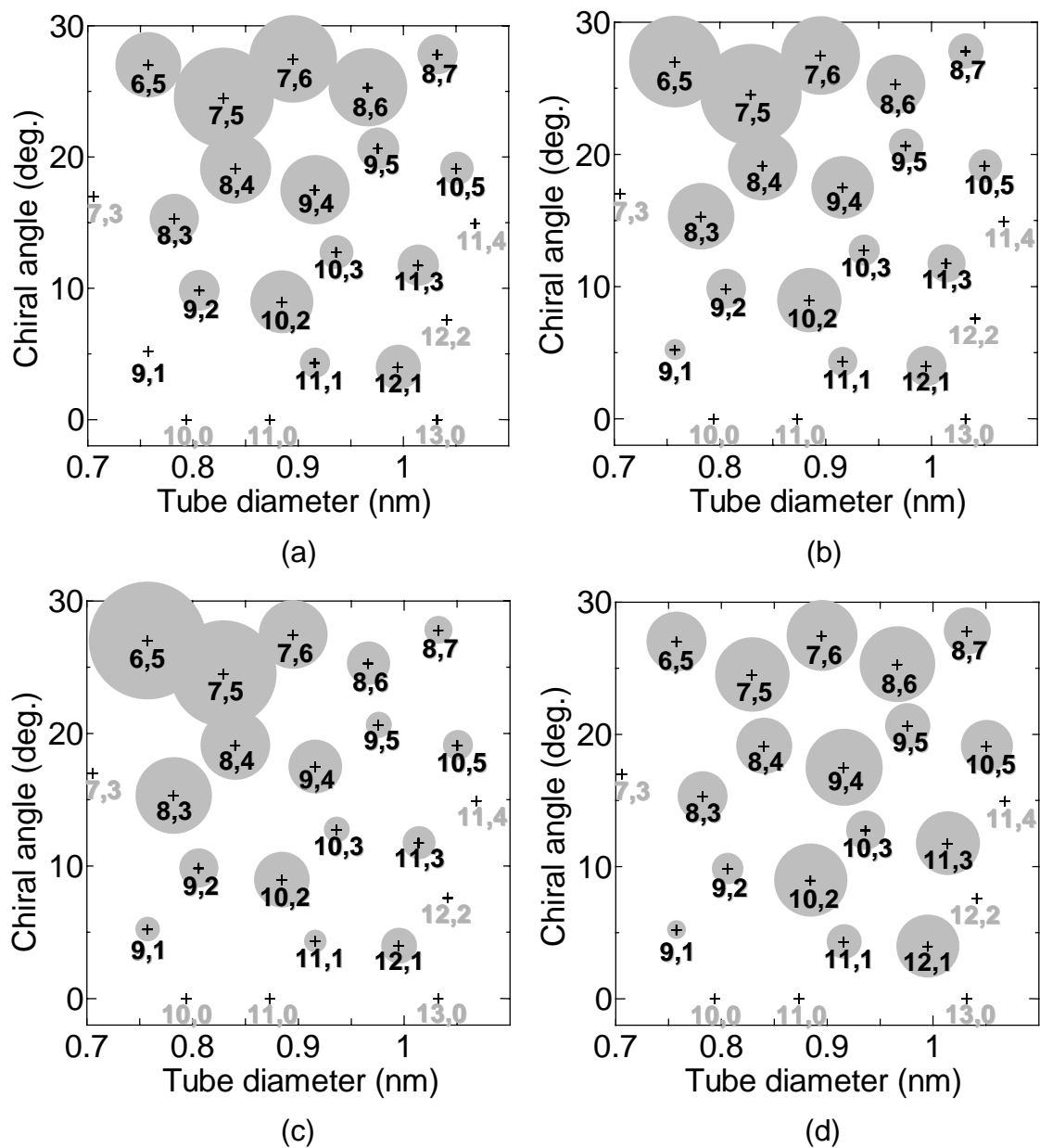


Fig. 3. Fluorescence intensity and chirality distributions of the ACCVD and HiPco samples shown in Fig. 2. The area of the circle at each (n, m) point denotes the measured relative emission intensity of the corresponding fluorescence peak.

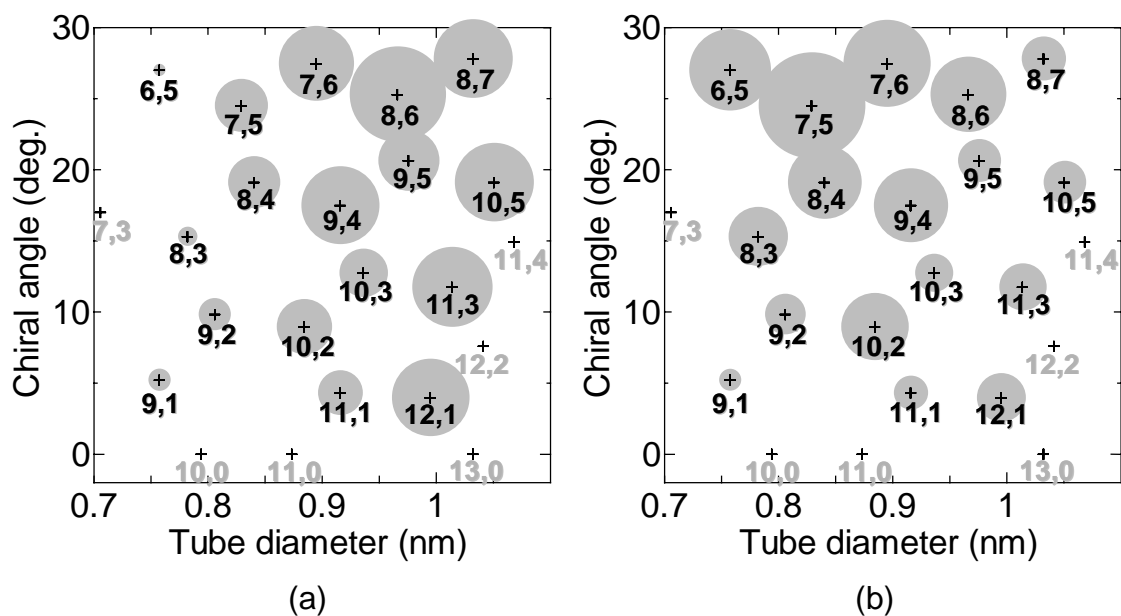


Fig. 4. Fluorescence intensity and chirality distribution of ACCVD SWNTs synthesized from different carbon sources and catalysts. (a) Synthesized from methanol instead of ethanol. (b) Synthesized using Co 5 wt % catalyst instead of Fe/Co 2.5 wt % catalyst. All other conditions were identical to the standard ACCVD at 850 °C.